Journal Homepage: http://ijcpe.uobaghdad.edu.iq
Iraqi Journal of Chemical and Petroleum Engineering
Vol. 25 No. 4 (December 2024) 107 – 114
EISSN: 2618-0707, PISSN: 1997-4884

Performance, Adsorption and Kinetic Study of AgY Zeolite for DBT Desulfurization

Radhaa Saeed [a, *], Tariq M. Naife [a], Mohammed Kadhim [b]

a Department of Chemical Engineering, College of Engineering, University of Baghdad, Baghdad, Iraq
b Leeds International Studygroup Centre, UK

Abstract

This study focuses on preparing and evaluating AgY zeolite as an adsorbent for the desulfurization (ADS) of dibenzothiophene (DBT) using a model fuel. Kinetic models and adsorption isotherms were investigated for this process. The AgY zeolite characterization was studied using XRD, BET, and XRF. XRD and XRF techniques revealed that AgY zeolite was successfully prepared with 21.42% wt. Ag. The BET results showed that the pore volume of AgY zeolite was 0.3596 cm^3/g and the surface area was 531 m^2/g. The desulfurization study was done with an initial sulfur content of 100–460 ppm. With 93% sulfur removal from the initial concentration of 100 ppm, ultra-deep desulfurization was achieved. The effect of contact time on the adsorption efficiency was investigated within a range of 10-120 min, and the results showed that most sulfur removal (52%) occurred after 10 minutes, while it reached 75% after 120 min with a sulfur capacity of 57.5 mg S/g. The results indicated that the Langmuir isotherm model was the most suitable to describe the process with R^2 of 99.29%, while the pseudo-second-order was the most fitted kinetic model to the data with R^2 of 98.57%.

Keywords: AgY Zeolite; Adsorptive Desulfurization; Adsorption isotherms; kinetic models.

Received on 08/10/2023, Received in Revised Form on 09/01/2024, Accepted on 11/01/2024, Published on 30/12/2024

https://doi.org/10.31699/IJCPE.2024.4.10

1- Introduction

Sulfur compounds are thought to be the primary source of atmospheric sulfur emissions, an environmental hazard located in crude oil. They are responsible for the deterioration of our environment, polluting the air, declining engine performance, and causing corrosion [1]. Based on the kind and origin of the crude oil, sulfur compounds can be found in crude oil in various forms and quantities, with concentrations ranging from trace levels to more than 8% wt.[2].

When sulfur and its derivatives in transportation fuels burn, they quickly turn into SO_2 and fine particles, which are airborne main toxins that damage the environment and social health by causing smog, acid rain, and dry depositions [3]. According to the World Health Organization, air pollution is the cause of three million deaths annually[4]. Environmental laws have been implemented in several nations worldwide to decrease sulfur content in fuel fractions to extremely minimal levels (10 parts per million). This has reduced the hazardous emissions from transportation fuel machines and improved air quality [5].

Hydrodesulfurization processes (HDS) need extremely harsh operating conditions, including pressures up to 10 MPa, temperatures as high as 400°C, a large quantity of catalyst, and a high hydrogen consumption rate. This is to remove heterocyclic complexes like DBT and its alkylated replacements, such as 4, 6-DMDBT. These heterocyclic sulfur compounds can be eliminated by the ADS process at mild conditions without expensive hydrogen [6,7]. The adsorptive desulfurization as a straightforward and ecologically friendly procedure is largely dependent on the adsorbent's textural characteristics. Pore volume, strong structural integrity, more mesoporous surface-active sites, and large surface area are the most important properties [8, 9].

The challenge is developing an adsorbent that can adsorb organosulfur better than other competitive hydrocarbons, specifically aromatics. It also needs to have a higher capacity for adsorption and regeneration so that it can be reused again. Numerous adsorbent types have been extensively studied in the literature, including activated carbon, metal oxides, supported metals, and metal-loaded zeolites [10]. Zeolites can be loaded with different metal ions, such as Ag^+, Zn^{2+}, Pd^{2+}, K^+, Cu^+, and Ni^{2+} using impregnation or ion-exchange methods. Modified zeolites with these metal ions increase their adsorption capacity and selectivity. Especially, Ag^+ and Pd^{2+} show a selectivity towards sulfur compounds in the presence of other compounds, such as aromatics, because of their selectivity towards polar particles and pore size [11]. The capacity of sulfur removal increased and the desulfurization efficiency was enhanced by the improved AgY [12–14].

*Corresponding Author: Email: radhaa.saeed1607m@coeng.uobaghdad.edu.iq

In this research, NaY zeolite was modified by loading Ag ions by batch ion exchange. The characterization of the adsorbent was performed by XRD, XRF, and BET. Then the removal of DBT from simulated fuel was studied at different parameters. Also, the adsorption kinetics and isotherms models were studied.

2- Experimental work

2.1. Materials

Table 1 shows all materials used for the experimental section of the research.

Table 1. The physical properties of the chemicals used in the current study

Material	Chemical Formula	Supplied Company	Origin	Molecular Weight	Phase
NaY Zeolite	N/A	ZR Catalyst CO., LTD	China	N/A	Solid powder
Silver Nitrate	$AgNO_3$	CARLO ERBA Reagents S.A.S	Italy	169.87 g/mol	Solid spheres
DBT	$C_{12}H_8S$	Fluka AG	Switzerland	184.26	solid
Cyclohexane	C_6H_{12}	Thomas Baker	India	84.16	liquid
Water	H_2O	Al-Joud	Iraq	18.015	Liquid

2.2. Preparation of modified AgY zeolite

AgY zeolite with specific metal loading percentages was obtained by adjusting the batch ion exchange technique according to the published research [15]. To achieve the necessary percentage of metal loading, 1 g of $AgNO_3$ was dissolved in distilled water (100 mL) using a conical flask connected to a reflux glass. NaY zeolite (provided by ZR Catalyst CO., LTD) was dried in an electric oven set to 90 °C for 4 h. Then 3 g of NaY zeolite was added to the silver solution. Due to $AgNO_3$ sensitivity to light, the entire procedure was carried out at midnight in an airtight and dark environment. The mixture was agitated for 6 h at 70°C at 450 rpm. After filtering, the suspension was thoroughly rinsed with deionized water and left to dry overnight at 80°C.

2.3. Experiments of desulfurization

Four model fuels containing different initial concentrations of sulfur (100-460) ppm were prepared by mixing cyclohexane with DBT. The batch experiment was run under stirring conditions at mild temperature, air pressure, and adsorbent particle size of (5-6 µm). To investigate the most fitted adsorption kinetic model isotherms, 0.3 g of the adsorbent was introduced to 50 ml of several model fuels for variable contacting time (10-120 min) and various initial sulfur concentrations (100-460 ppm). Also, 0.3 g of commercial NaY zeolite was introduced to 50 ml of model fuel containing 460 ppm of sulfur for 120 min to measure its sulfur saturation capacity. The adsorbent was used in powder form. The fuel was stirred at 450 rpm for a varied contact duration. After using a vacuum pump to separate the fuel from the powder, the mixture was sent for a sulfur content measuring test.

Removal of sulfur was shown as Desulfurization efficiency (DS%) which is calculated as the ratio of sulfur removed to that initially present in the fuel.

$$DS\ \% = \frac{C_o - C}{C_o} * 100 \quad (1)$$

Where: C_o: the initial sulfur content in fuel. C: the measured sulfur content in fuel.

To determine the adsorption capacity, Eq. 2 and Eq. 3 were used:

$$qe = \frac{Co - Ce}{m} x\ V \quad at\ an\ equilibrium\ time \quad (2)$$

$$qt = \frac{Co - Ct}{m} x\ V \quad at\ different\ mixing\ time \quad (3)$$

Where: q_e: adsorption capacity at equilibrium mg/g. q_t: adsorption capacity at sampling time mg/g. V: volume of model fuel in L. M: mass of adsorbent in g. C_o, C_e, and C_t are sulfur content at initial, equilibrium, and intervals sampling time respectively in mg/L.

2.4. Techniques of characterization

The crystal structure of NaY and AgY zeolites was studied using Cu-Kα radiation as the X-ray source and a λ value of 1.54056 °A, a 2theta range of 5 to 80, and the Pananylatical Aeris X-ray diffraction model. The nitrogen adsorption-desorption isotherm (the Brunauer Emmett teller BET method) was employed to measure surface area and pore volume (Micrometrics, ASAP, 2020, USA). The elemental structure of NaY and AgY zeolites was determined using the X-ray fluorescence (XRF) device (Spectro Xepos, Ametek, Germany). ASTM D7039 was used to measure the total sulfur contents of the model fuel samples that were treated and the standard samples.

3- Results and discussion

3.1. Characterization of adsorbent

3.1.1. X-Ray diffraction analysis (XRD)

Comparing the XRD patterns of a commercial NaY zeolite with modified zeolites (AgY) is illustrated in Fig. 1. The exact peaks of the commercial Y zeolite [6.3° (1 1 1), 15.9◦ (3 3 1), 20.7° (4 4 0), 24.0° (5 3 3), 27.5° (6 4 2), and 31.9° (5 5 5)] appeared in the AgY XRD patterns. The modification did not affect the zeolite structure as shown by the XRD pattern and clean peaks that distinguish the pure phase of the Y zeolite. The peak at 38° indicates that there is a small quantity of Ag_2O present, and the ion-exchange process loaded silver metal onto the zeolite these findings are consistent with earlier research [15, 16].

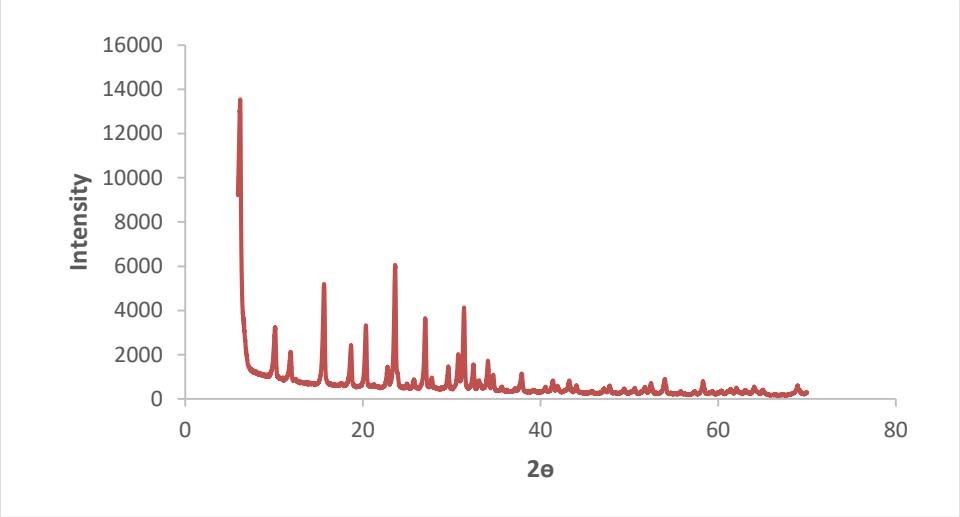

Fig. 1. XRD analysis of modified AgY zeolite

3.1.2. N_2 adsorption-desorption isotherm

The results of the N_2 adsorption-desorption isotherm of AgY and Na Y zeolites are shown in Table 2. The pore volume of AgY zeolite (0.3596 cm^3/g) was higher than that of NaY zeolite (0.278 cm^3/g) but the crystalline structure remained intact, and the surface area of NaY zeolite (703.04 m^2/g) was larger than of the AgY zeolite (531 m^2/g). This may be because of the ion exchange process's delamination and integration of Ag ions into the zeolite's structure. This behavior is consistent with zeolite delamination found in earlier research [17]. The ionic radius of silver (0.15 nm) is larger than that of Na (0.1 nm) which may cause a little expansion of the zeolite lattice and an increase in pore volume. Similar results were shown in an earlier study [18] when NaY zeolite ions exchanged with nickel ions.

3.1.3. X-ray fluorescence (XRF)

The required Ag loading percentage on the zeolite was given by the XRF analysis conducted for the modified AgY zeolite and commercial NaY zeolites shown in Table 2. The analysis reveals that the zeolite's Si/Al molar ratio was in the range of NaY zeolite, indicating that the adsorbent crystals were not affected by ion exchange and thermal treatment. The result was consistent with [19].

Table 2. Structure properties of adsorbents obtained by the BET and XRF

Adsorbent	Surface area (m^2/g)	Pore volume (cm^3/g)	Ag% wt.	Si/Al
NaY	703.04	0.2780	0	2.65
AgY	531	0.3596	21.42	3.053

3.2. Performance evaluation of adsorption desulfurization process

3.2.1. Effect of sulfur initial concentration

Initial sulfur concentration was studied to determine the best adsorption isotherms to describe the adsorption experiments. For desulfurization over AgY zeolite, the removal of sulfur efficiency decreased with rising sulfur content in model fuel. As shown in Fig. 2, deep-ultra desulfurization was achieved for 100 ppm of sulfur and the final concentration was below 10 ppm while the efficiency for 100, 200, 300, and 460 ppm concentrations of sulfur decreased as follows: 93%, 88%, 81%, and 75% respectively. AgY zeolite showed a sulfur saturation capacity of 57.5 mg S/g adsorbent while NaY zeolite exhibited only 18.4 mg S/g adsorbent. While the sulfur initial concentration was raised, the number of active sites of the adsorbent was still constant. Therefore, the sulfur atoms quantity was in excess, and further removal beyond the saturation point couldn't be applied. These results agreed with Thaligari [20].

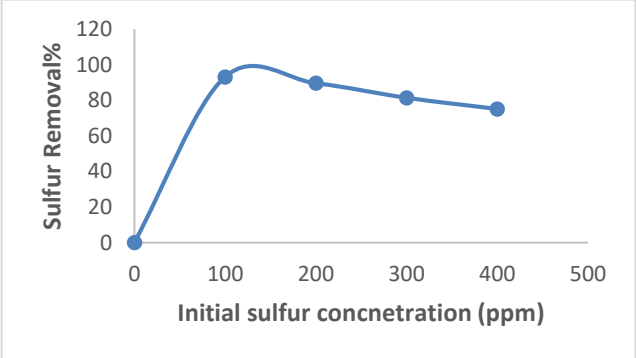

Fig. 2. The relation between initial sulfur concentration and removal efficiency of DBT by AgY zeolite (0.3 g/50 ml, t=120 min, AS= 450 rpm, T= 25°C)

3.2.2. Effect of contact time

Sulfur removal was studied at different concentrations. It is clear from Fig. 3 that most of the removal happened after 10 min for AgY zeolite (52%). AgY zeolite sulfur saturation capacity was raised until equilibrium reached 60 min and no additional reasonable desulfurization was seen. According to Song [19], the adsorbent active sites are gradually engaged with the sulfur compound for a predetermined contact duration until the saturation capacity is attained, and the maximum adsorption occurs.

Regardless of increasing the contact duration, no noticeable desulfurization happened.

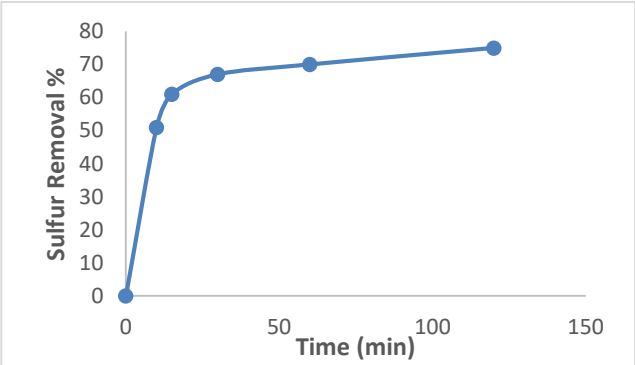

Fig. 3. The effect of contact time on desulfurization of DBT by AgY zeolite (m= 0.3g/50 ml, T= 25 ºC, AS= 450 rpm, Sulfur Content= 460 ppm)

3.3. Adsorption isotherms models

The relation between the adsorbent's quantity (q_e) and the remaining concentration of the adsorbate (C_e) at equilibrium state and constant temperature was described by the adsorption isotherms [3]. The advantage of using adsorption isotherm is to fully understand the relation of the contacting mechanism between the dissolved compounds and the adsorbent in the solution[21]. Furthermore, adsorption isotherms deliver a demonstration of how molecules are distributed in a liquid medium and solid phase when an equilibrium state is achieved during the adsorption process [22].

3.3.1. Langmuir model

In 1916 Irving Langmuir proposed this isotherm which describes the adsorption as one layer and the energy distributed on the adsorbent surface. Langmuir isotherm assumes the process of adsorption is limited to only monolayer surface, and the adsorption sites are identical and restricted to a specific number. Also, the highest adsorption is reached when the primary layer is saturated with adsorbate ions. Lastly, the adsorption occurs in uniform case. The mathematical equations that describe Langmuir adsorption isotherm in the nonlinear and linear forms are listed below [23–25]:

$$q_e = \frac{q_{max} K_L C_e}{1 + K_L C_e} \quad (4)$$

$$\frac{1}{q_e} = \frac{1}{q_{max} K_L} \frac{1}{C_e} + \frac{1}{q_{max}} \quad (5)$$

Where: q_e: adsorption capacity when equilibrium is achieved (mg/g). C_e: the adsorbed concentration at equilibrium (mg/l). q_{max}: adsorption capacity at maximum (mg/g). K_L: Langmuir constant expressed the binding sites (l/mg).
If $K_L C_e$ is smaller than unity, then the obtained adsorption isotherm is linear. For modest amounts of adsorption $q_e = q_{max} K_L C_e$. If $K_L C_e$ is bigger than unity, then $q_e = q_{max}$.

3.3.2. Freundlich model

Freundlich isotherm was the first model derived for explaining adsorption isotherms. Herbert Freundlich established this model in 1909 assuming the surface of adsorbent is heterogeneous, and the active sites and energy are equivalent. In addition, it assumed the adsorbent molecules can attract each other, but the attraction is not significant enough to predicate the maximum limits of adsorption. Eq. 6 shows the nonlinear form of the isotherm. Whereas Eq. 7 shows the linear form of the isotherm model [23–25]:

$$q_e = K_F C_e^{\frac{1}{n}} \quad (6)$$

$$\ln q_e = \ln K_F + \frac{1}{n} \ln C_e \quad (7)$$

Where: K_F: is known as the Freundlich constant which represents the calculated capacity of adsorption $[(mg.g^{-1}).(mg^{-1})^{1/n}]$. n: is the intensity value for adsorption which determines the adsorption type.

3.3.3. Timken model

This model was proposed by Russian scientist Mikhail Temkin in 1940. The Temkin model assumes that when the number of molecules presenting in the adsorption layer of a solid surface increases, the adsorption temperature decreases linearly rather than logarithmically. This model is also applicable to complex liquid-phase adsorption systems because of its remarkable ability to predict gas-phase equilibrium. Eq. 8 shows the nonlinear form of the model, and Eq. 9 shows the linear form of the Temkin isotherm model [23–25]:

$$q_e = \frac{RT}{b} \ln K_T C_e \quad (8)$$

$$q_e = B \ln K_T + B \ln C_e \quad (9)$$

$$B = \frac{RT}{b} \quad (10)$$

Where: R: is the universal constant of gases (8.3144 J/mol. K). T: is the temperature in absolute value (Kelvin). K_T: is the binding constant of the Timken isotherm at equilibrium (L/g). B: is a constant of the model

Fig. 4 to Fig. 6 shows the application of Eqs. 5, 7, and 9 and the parameters and correlation factors of each adsorption isotherm are shown in Table 3.

The data shown in Table 3 indicate that the Langmuir isotherm was the most suitable for describing the experiments of DBT adsorptive desulfurization by AgY zeolite because its R^2 value was 99.29% which is close to unity. The Langmuir isotherm described the presence of a monolayer of the adsorbate (DBT) at the surface of the adsorbent for the given concentration range. According to Al-Ghouti [22], the Langmuir adsorption isotherm assumes there is a monolayer homogenous adsorption on the adsorbent surface. The value of n calculated from the Freundlich adsorption isotherm equation was 2.199.

According to recent research [3], the value of n in the range of 2-10 indicates good physical adsorption, in the range of 1-2 indicates some adsorption difficulty, and unfavorable adsorption if n is lower than unity.

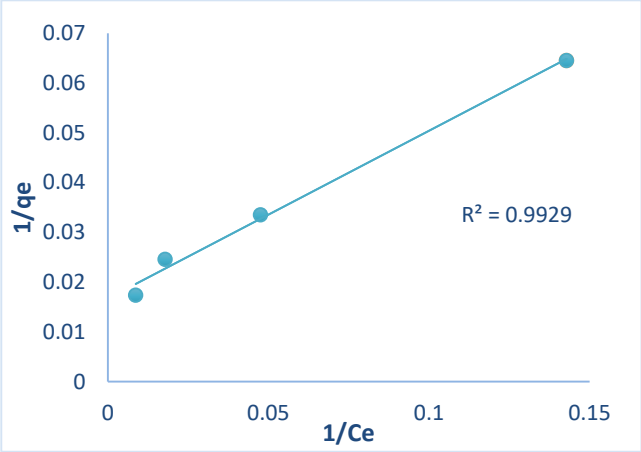

Fig. 4. Langmuir adsorption isotherm plot

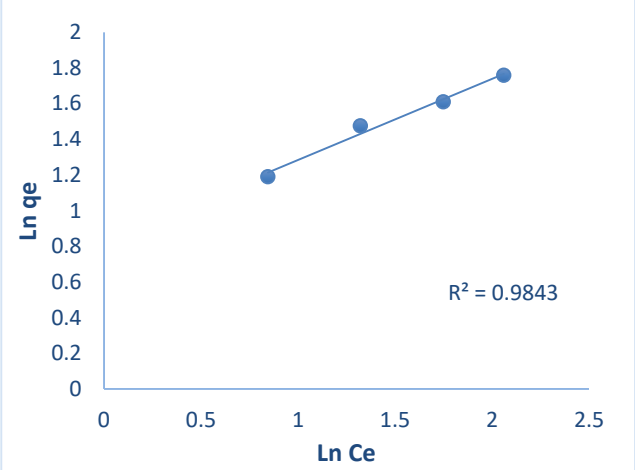

Fig. 5. Freundlich adsorption isotherm plot

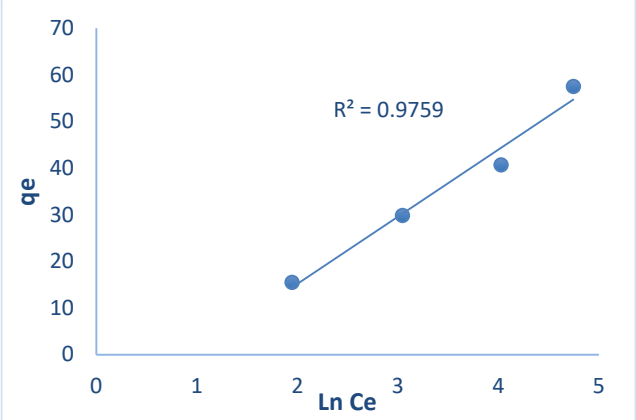

Fig. 6. Temkin adsorption isotherm plot

These data showed that the experimental results fitted these models as follows: Langmuir model > Freundlich model > Temkin model.

3.4. Adsorption kinetics

Adsorption kinetic is the rate at which pollutants travel from the liquid phase to the adsorbent surface at specific values of variables. The pseudo-first-order and pseudo-second-order are the dominant models and the most applied to study the adsorption kinetics [25].

3.4.1. Pseudo-first order model

In 1898, Sten Yangve Dennis, who is a Swedish physicist, proposed this model. Adsorption was assumed to form in one layer on the surface of adsorption between liquid and solid phases. Also, pseudo-first order was used to illustrate the first periods of adsorption phenomena. The following linear Eq. 11 represents this model [26–29].

$$ln\,(q_e - q_t) = ln\,q_e - k_1 t \quad (11)$$

Where: k_1: is the constant rate (1/min)

Table 3. The constants of adsorption isotherms model

Langmuir model			Freundlich model			Temkin model		
K_L	q_m	R^2	K_F	n	R^2	B	K_T	R^2
0.049	57.5	99.29%	6.7499	2.199	98.43%	14.4	2.583	97.59%

3.4.2. Pseudo-second order

The pseudo-second-order kinetic model is applied to demonstrate the fully achieved process of adsorption and the total quantity of adsorption. It was assumed that the amount adsorbed on the adsorbent surface at equilibrium is proportional to the reaction speed. Also, the amount of surface active sites that are accessible has a relation to the adsorption rate [26–29]. The linearized form of the pseudo-second-order model is shown in Eq. 12.

$$\frac{t}{q_t} = \frac{1}{k_2 q_e^2} + \frac{1}{q_e} t \quad (12)$$

Where: K_2: is the constant rate (1/min).

The kinetic data of adsorption of DBT on AgY zeolite adsorbent have been calculated using two models the pseudo-first order and pseudo-second order models. Table 4 lists the correlation factors and other parameters belonging to the two applied models. From Fig. 7 and Fig. 8, the pseudo-second-order was the best model to represent the experimental data as it had the highest correlation factor which was very close to unity (98.57%). According to previous studies [19, 31, 32], pseudo-second-order is the suitable model to describe the adsorptive desulfurization of organosulfur compounds in the presence of pi complexation chemisorption.

Table 4. The Parameters of Pseudo-First Order Model and Pseudo-Second Order Model

Pseudo- first order model			Pseudo- second order model		
q_e	K_1	R^2	q_e	K_2	R^2
38.0005	00038	97.59%	67.11	0.00811	97.59%

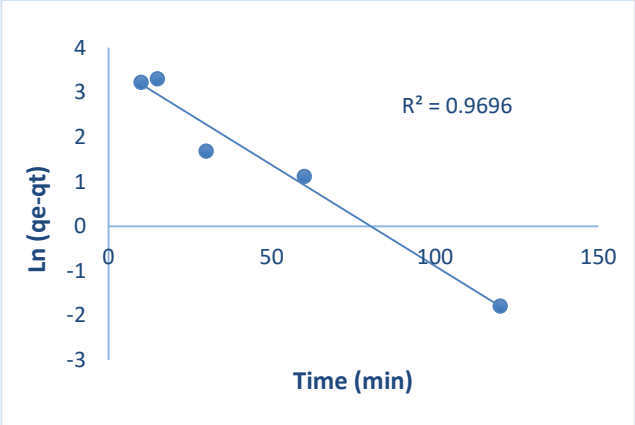

Fig. 7. The pseudo- first order kinetic model plot

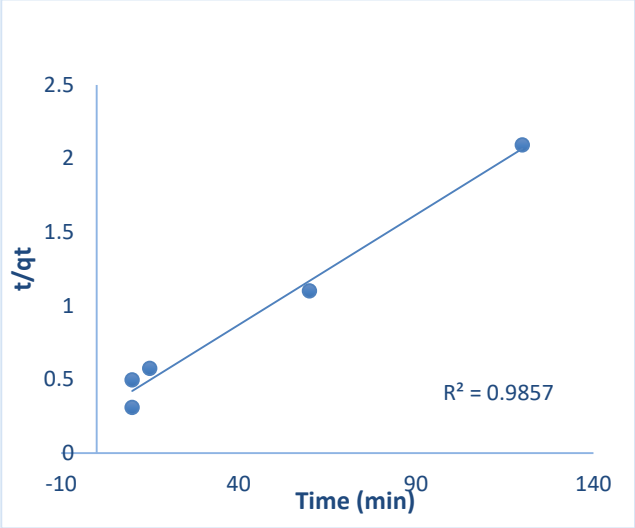

Fig. 8. The pseudo- second order kinetic model plot

4- Conclusions

Modification of NaY zeolite to obtain AgY zeolite was successfully achieved with an Ag content of 21.42%. The modification did not affect the structure of zeolite according to the XRD results. AgY zeolite showed an acceptable surface area of 531 m^2/g and a pore volume of 0.3596 cm^3/g. AgY zeolite achieved a high DBT removal efficiency of 93% for a feed containing 100 ppm. The experimental results of DBT adsorption by AgY zeolite were successfully described by the Langmuir isotherm model and the pseudo-second-order model confirming the monolayer chemical adsorption.

References

[1] A.-H. A. Mohammed and M. A. Abdulwahhab, "Naphtha desulfurization by prepare Cu-Ni-zeolite adsorbent," *Iraqi Journal of Chemical and Petroleum Engineering*, vol. 15, no. 4, pp. 9–14, 2014, https://doi.org/10.31699/IJCPE.2014.4.2

[2] B. Radhi and W. Mohammed, "TiO2 loading on activated carbon: preparation, characterization, desulfurization performance and isotherm of the adsorption of dibenzothiophene from model fuel," *Egyptian Journal of Chemistry*, vol. 66, no. 7, pp. 428-437, 2023, https://doi.org/10.21608/ejchem.2022.109702.5003

[3] B. D. Radhi and W. T. Mohammed, "Novel nanocomposite adsorbent for desulfurization of 4,6-dimethyldibenzothiophene from model fuel," *Materials Today: Proceedings*, vol. 42, pp. 2880–2886, 2021, https://doi.org/10.1016/j.matpr.2020.12.738

[4] X. Sun and B. Tatarchuk, "Photo-assisted adsorptive desulfurization of hydrocarbon fuels over TiO2 and Ag/TiO2," *Fuel*, vol. 183, pp. 550–556, 2016, https://doi.org/10.1016/j.fuel.2016.06.072

[5] M. M. Yahya and H. Q. Hussein, "Adsorption Desulfurization Of Iraqi Heavy Naphtha Using Zeolite 13x," *Association of Arab Universities Journal of Engineering Sciences*, vol. 26, no. 2, pp. 12–18, 2019, https://doi.org/10.33261/jaaru.2019.26.2.003

[6] G. K. Jabaar, H. A. Al-jendeel, and Y. Ali, "Desulphurization of Simulated Oil Using SAPO-11 with CNT 's as Adsorbent : A Kinetic Study," *Iraqi Journal of Chemical and Petroleum Engineering,vol*. 24, no. 3, pp. 69–77, 2023, https://doi.org/10.31699/IJCPE.2023.3.7

[7] S. Kumar, N. S. Bajwa, B. S. Rana, S. M. Nanoti, and M. O. Garg, "Desulfurization of gas oil using a distillation, extraction and hydrotreating-based integrated process," *Fuel*, vol. 220, no. December 2017, pp. 754–762, 2018, https://doi.org/10.1016/j.fuel.2018.02.041

[8] M. A. Betiha, A. M. Rabie, H. S. Ahmed, A. A. Abdelrahman, and M. F. El-Shahat, "Oxidative desulfurization using graphene and its composites for fuel containing thiophene and its derivatives: An update review," *Egypian Journal of Petroleum*, vol. 27, no. 4, pp. 715–730, 2018, https://doi.org/10.1016/j.ejpe.2017.10.006

[9] B. Dutta, "Principles of mass transfer and seperation procesess", PHI Learning, New Delhi, India, 2009.

[10] H. J. Mousa and H. Q. Hussein, "Adsorptive Desulfurization of Iraqi Heavy Naphtha Using Different Metals over Nano Y Zeolite on Carbon Nanotube," *Iraqi Journal of Chemical and Petroleum Engineering*, vol. 21, no. 1, pp. 23–31, 2020, https://doi.org/10.31699/ijcpe.2020.1.4

[11] R. Dehghan and M. Anbia, "Zeolites for adsorptive desulfurization from fuels: A review," *Fuel Process Technology*, vol. 167, pp. 99–116, 2017, https://doi.org/10.1016/j.fuproc.2017.06.015

[12] D. T. Tran, J. M. Palomino, and S. R. J. Oliver, "Desulfurization of JP-8 jet fuel: challenges and adsorptive materials," *RSC Advances*, vol. 8, no. 13, pp. 7301–7314, 2018, https://doi.org/10.1039/C7RA12784G

[13] A. J. Hernández-Maldonado and R. T. Yang, "Desulfurization of commercial liquid fuels by selective adsorption via π-complexation with Cu(I)-Y zeolite," *Industrial & Engineering Chemistry Research.*, vol. 42, no. 13, pp. 3103–3110, 2003, https://doi.org/10.1021/ie0301132

[14] S. M. Al-Jubouri, "The static aging effect on the seedless synthesis of different ranges FAU-type zeolite Y at various factors," *Iraqi Journal of Chemical and Petroleum Engineering*, vol. 20, no. 4, pp. 7–13, 2019, https://doi.org/10.31699/ijcpe.2019.4.2

[15] S. M.AL-Jubori, H. Sabbar, E. Khudhair, S. H. Ammar, S. Al Batty, S. Y. Khudhair, A. S Mahdi, "Silver oxide-zeolite for removal of an emerging contaminant by simultaneous adsorption-photocatalytic degradation under simulated sunlight irradiation," *Journal of Photochemistry and Photobiology A: Chemistry*, vol. 442, no. February, p. 114763, 2023, https://doi.org/10.1016/j.jphotochem.2023.114763

[16] M. Abdullah and S. Al-Jubouri, "Implementation of hierarchically porous zeolite-polymer membrane for Chromium ions removal," *IOP Conference Series: Earth and Environmental Science*, vol. 779, no. 1, 2021, https://doi.org/10.1088/1755-1315/779/1/012099

[17] S. Nuntang, P. Prasassarakich, and C. Ngamcharussrivichai, "Comparative study on adsorptive removal of thiophenic sulfurs over Y and USY zeolites," *Industrial & Engineering Chemistry Research*, vol. 47, no. 19, pp. 7405–7413, 2008, https://doi.org/10.1021/ie701785s

[18] N. S. Ahmedzeki and B. A. Al-Tabbakh, "Catalytic Reforming of Iraqi Naphtha over Pt-Ti / HY Zeolite Catalyst," *Iraqi Journal of chemical and Petroleum Engineering*, vol. 17, no. 3, pp. 45–56, 2016, https://doi.org/10.31699/IJCPE.2016.3.4

[19] H. Song, X. Wan, and X. Sun, "Preparation of Agy zeolites using microwave irradiation and study on their adsorptive desulphurisation performance," *The Canadian Journal of Chemical Engineering*, vol. 91, no. 5, pp. 915–923, 2013, https://doi.org/10.1002/cjce.21736

[20] S. K. Thaligari, V. C. Srivastava, and B. Prasad, "Adsorptive desulfurization by zinc-impregnated activated carbon: characterization, kinetics, isotherms, and thermodynamic modeling," *Clean Technology and Environmental Policy*, vol. 18, no. 4, pp. 1021–1030, 2016, https://doi.org/10.1007/s10098-015-1090-y.

[21] N. Gaur, K. Narasimhulu, and Y. PydiSetty, "Recent advances in the bio-remediation of persistent organic pollutants and its effect on environment," *Journal of Cleaner Production*, vol. 198, pp. 1602–1631, 2018, https://doi.org/10.1016/j.jclepro.2018.07.076

[22] M. A. Al-Ghouti and D. A. Da'ana, "Guidelines for the use and interpretation of adsorption isotherm models: A review," *Journal of Hazardous Materials*, vol. 393, no. November 2019, p. 122383, 2020, https://doi.org/10.1016/j.jhazmat.2020.122383

[23] S. A. Obaid, "Langmuir, Freundlich and Tamkin Adsorption Isotherms and Kinetics for the Removal Aartichoke Tournefortii Straw from Agricultural Waste," *Journal of Physics: Conference Series*, vol. 1664, no. 1, 2020, https://doi.org/10.1088/1742-6596/1664/1/012011

[24] J. Wang and X. Guo, "Adsorption isotherm models: Classification, physical meaning, application and solving method," *Chemosphere*, vol. 258, p. 127279, 2020, https://doi.org/10.1016/j.chemosphere.2020.127279

[25] S. V. dos S. Barbosa, "Adsorption equilibrium and fixed-bed adsorption of phenolic acids onto polymeric adsorbent," pp. 1–70, 2015.

[26] X. Chen, "Modeling of experimental adsorption isotherm data," *Information*, vol. 6, no. 1, pp. 14–22, 2015, https://doi.org/10.3390/info6010014

[27] E. D. Revellame, D. L. Fortela, W. Sharp, R. Hernandez, and M. E. Zappi, "Adsorption kinetic modeling using pseudo-first order and pseudo-second order rate laws: A review," *Cleaner Engineering and Technology*, vol. 1, no. October, p. 100032, 2020, https://doi.org/10.1016/j.clet.2020.100032

[28] S. Shah, I. Ahmad, W. Ahmad, M. Ishaq, K. Gul, R. Khan, H. Khan., "Study on adsorptive capability of acid activated charcoal for desulphurization of model and commercial fuel oil samples," *Journal of Environmental Chemical Engineering*, vol. 6, no. 4, pp. 4037–4043, 2018, https://doi.org/10.1016/j.jece.2018.06.008

[29] A. E. Rodrigues and C. M. Silva, "What's wrong with Lagergreen pseudo first order model for adsorption kinetics?," *Chemical Engineering Journal*, vol. 306, no. August, pp. 1138–1142, 2016, https://doi.org/10.1016/j.cej.2016.08.055

[30] P. Sikarwar, U. K. A. Kumar, V. Gosu, and V. Subbaramaiah, "Synergetic Effect of Cobalt-Incorporated Acid-Activated GAC for Adsorptive Desulfurization of DBT under Mild Conditions," *Journal of Chemical and Engineering Data*, vol. 63, no. 8, pp. 2975–2985, 2018, https://doi.org/10.1021/acs.jced.8b00249

[31] L. M. Lalitha and S. Mariraj Mohan, "Performance evaluation of multibed adsorbent on removal of hexavalent chromium through various kinetic models," *Journal of Environmental Engineering and Landscape Management*, vol. 26, no. 4, pp. 285–298, 2018, https://doi.org/10.3846/jeelm.2018.6269

دراسة الاداء والامتزازية والحركية لالزالة مركب الكبريت العضوي من محاكاة وقود النقل باستخدام مادة الفضة/ زيولايت

رضاء نزار سعيد [١، *]، طارق محمد نايف [١]، محمد عبدالاله كاظم [٢]

١ قسم الهندسة الكيمياوية، كلية الهندسة، جامعة بغداد، بغداد، العراق
٢ مركز ليدز الدولي للدراسات، المملكة المتحدة

الخلاصة

هذه الدراسة تركز على تحضير وتقييم مادة AgY زيولايت كمادة مازة تستخدم في عملية ازالة الكبريت الامتزازية لازالة مركب الكبريت العضوي DBT من محاكاة وقود النقل. كما تم دراسة الموديلات الحركية لعملية الامتزاز. XRD, BET, XRF هي التقنيات التي استخدمناها خلال البحث لتشخيص خصائص الزيولايت وقد تبين من هذه التقنيات نجاح عملية تحميل ايونات الفضة على الزيولايت وبنسبة ٢١,٢٤% وبحجم مسامي بلغ ٠,٣٥٩٦ سم^3 /غم ومساحة سطحية ٥٣١ م^2/ غم. تم دراسة عملية ازالة الكبريت مع تركيز كبريت ابتدائي يتراوح من 100–460 ppm . تم تحقيق ازالة الكبريت العميقة عند تريكز كبريت ابتدائي 100 ppm ثم تم دراسة تأثير زمن التلامس على عملية الامتزاز بمدى يتراوح من ١٠ الى ١٢٠ دقيقة حيث تبين الكمية الاكبر للازالة حصلت في العشر دقائق الاولى من العملية (٥٢%) بينما وصلت نسبة الازالة الى ٧٥% بعد ١٢٠ دقيقة ووصلت سعة الامتزاز الى ٥٧,٥ ملغم كبريت/ غم من المادة المازة. وبعد ان جمعنا البيانات المطلوبة في المختبر تم تحليل عملية الامتزاز لايجاد الموديلات الافضل وصفا للعلمية. لقد بينت النتائج ان موديل Langmuir هو الموديل الاكثر تطابقا لوصف العملية R^2=99.29% وان الموديل pseudo من المرتبة الثانية هو الافضل لوصف الحركية حيث بلغ R^2= 98.57%.

الكلمات الدالة: زيولايت AgY، ازالة الكبريت بالامتزاز، الايزوثرمية للامتزاز، الموديلات الحركية.